https://dx.doi.org/10.1016/j.ijrmhm.2021.105673

Wear-resistance enhancement of nanostructured W-Cu-Cr composites

Lijun Cao[a], Chao Hou[a], Fawei Tang[a], Tielong Han[a], Xintao Huang[a], Yurong Li[a], Gaochao Wu[b], Chao Liu[b], Shuhua Liang[c], Junhua Luan[d], Zengbao Jiao[e], Zuoren Nie[a], Xiaoyan Song[a]

a Faculty of Materials and Manufacturing, Key Laboratory of Advanced Functional Materials, Ministry of Education of China, Beijing University of Technology, Beijing 100124, China
b Xiamen Tungsten Co., Ltd., Xiamen 361009, China
c College of Materials Science and Engineering, Shaanxi Province Key Laboratory of Electrical Materials and Infiltration Technology, Xi'an University of Technology, Xi'an 710048, China
d Department of Materials Science and Engineering, City University of Hong Kong, Hong Kong, China
e Department of Mechanical Engineering, The Hong Kong Polytechnic University, Hong Kong, China

Abstract
Nanostructured W-Cu-Cr composites were fabricated, which exhibit exceptionally high hardness (~1000 HV) as compared with those of the conventional W-Cu composites, due to the combined advantages of Cr dissolution, precipitate formation and grain refinement. Nonmonotonic variation of the wear resistance with hardness was discovered. With an appropriate content of Cr, the preferential oxidation reduced the oxidation of W. Moreover, it facilitated formation of a stable protective film with fish-scale morphology and also refined the structure, leading to a high microhardness at the worn surface. The wear rate (1.65 × 10−6 mm3 N−1 m−1) was reduced by an order of magnitude compared with that of the conventional counterpart. However, excessive addition of Cr may deteriorate the wear resistance in spite of a higher hardness due to the embrittlening of W phase and difficulty to form a stable protective film at the worn surface. This study provides a new strategy for developing W-Cu composites with outstanding wear resistance.

Keywords: W-Cu based composite; Nanostructure; Hardness; Wear resistance

1. Introduction
W-Cu composites are widely applied in the aerospace fields and civilian industries, such as electrical power systems, missile nozzles and electromagnetic guide rail, taking combined advantages from high melting point, high strength and hardness of W as well as excellent thermal and electrical conductivity of Cu [[1], [2], [3], [4]]. Under some critical service conditions, the W-Cu composites have to bear harsh wear processes with complex mechanical and thermal interactions induced by heavy load, fast sliding speed and high temperature [5]. Therefore, requirements for greatly improved mechanical

properties in terms of high hardness and wear resistance are put forward, and these are critical for the outstanding reliability and durability of W-Cu composites [[6], [7], [8]]. The wear resistance of composites is related to not only the pristine hardness [9], but also the evolved microstructure beneath the worn surface during the wear process [[10], [11], [12], [13]]. The composites with higher hardness can have shallower indentation depth and smaller grinding volume under wear conditions [14]. Thus a material with a higher hardness generally exhibits better wear resistance. Most studies have improved the wear resistance of composites by refining grain size [15,16] and introducing dispersive nanoparticles [[17], [18], [19]]. Although the nanoparticles can refine the microstructure, the grain sizes of the W-Cu based composites are mostly on the micron scale due to utilization of initial raw powders with coarse particle size and also rapid grain growth during the powder densification process [20,21]. Therefore, to improve the wear resistance fundamentally by the roots, it is of great significance to develop the nanostructured W-Cu composites by controlling the grain coarsening in the fabrication process [22,23] and also to enhance the thermal stability of the nanostructure [[24], [25], [26]].

Up to now, a lot of efforts have been paid to develop submicron and nanostructured W-Cu based composites [[27], [28], [29], [30], [31]]. The wear resistance of such nanostructured composite was obviously improved compared with that of the conventional coarse-grained counterpart [32]. In our previous work, in order to stabilize the nanostructures in the W-Cu composite at high temperature, we proposed a strategy to fabricate nanostructured W-Cu based composites by in-situ solid-state reactions [33]. The in-situ formed hard Cr and WC particles played an important role in pinning the migration of interfaces [34]. Further, strong interfacial combination between matrix and hard particles was maintained after wear tests. These factors resulted in the restriction of formation of the mechanical mixed layer (MML) and the delamination, thus altering the dominant wear mode to the single abrasive wear. Consequently, the wear resistance of the composite was significantly boosted.

In another work, a high hardness of 650 HV was achieved in an equiatomic TiMoNb alloy through segregation of solute atoms and formation of precipitates coherent with the matrix [35]. The refined microstructure and stabilized interfaces induced a high wear resistance both at room and high temperatures. Considering the important effect of microstructure in the W skeleton on the mechanical property of W-Cu composite [36], it is necessary to stabilize the nanostructure inside the W phase and strengthen the interfacial bonding [37]. Furthermore, it needs to explore the changing tendency of wear resistance with microstructural evolution, and effects of oxidation and mechanical properties of the worn surface on the wear resistance. These will provide deep insight in developing W-Cu composite with excellent wear resistance.

In this work, nanostructured W-Cu-Cr composites have been fabricated, it is found that at a certain Cr content, the hardness of the W-Cu-Cr composite can be improved to as high as 1085 HV. This indicates a significant hardening effect of Cr on the W-Cu composites. However, it is discovered that the wear resistance does not have a monotonously increasing relationship with the increment of hardness. Further, the evolution of the morphology, composition and microstructure of the worn surface of

the nanostructured W-Cu-Cr composite will be investigated to reveal mechanisms of the wear resistance. This study may provide important guidance for achieving high wear resistance that is applicable to various metallic composites.

2. Experimental

The raw materials of W (particle size <2 μm), Cr (average particle size of 700 nm) and Cu (particle size <2 μm) powders were adopted. The content of Cu in all samples was unified to be 20 wt%. A series of Cr contents of 2 wt%, 4 wt%, 6 wt% and 10 wt% were introduced in the composites, noted as W-Cu-2Cr, W-Cu-4Cr, W-Cu-6Cr and W-Cu-10Cr, respectively. A two-step ball milling procedure was used to make the powder mixture. Specifically, the W and Cr powders were firstly dry-milled with a higher rotation speed of 500 rpm for 48 h to form W-Cr solid solution powder. Then, Cu powder was added into the W-Cr powder by milling with a lower rotation speed of 300 rpm and liquid medium of ethanol. The milling tank and balls are made of cemented carbides to avoid metallic impurities, such as Fe. The powder mixture was sintered by spark plasma sintering (SPS) to fabricate the bulk material with a diameter of 20 mm and thickness of several millimeters. The sintering was carried out in vacuum of ~2×10^{-2} Pa. The sintering temperatures were set as 955 °C for the W-Cu-10Cr and 970 °C for the other composites. The holding time, heating rate and pressure were 5 min, 100 °C min^{-1} and 100 MPa, respectively. More detailed experimental procedures can be acquired in our previous work reported in the literature [38]. A commercial W-20wt.%Cu bulk composite with an average size of W phase as about 5 μm (noted as coarse-grained W-Cu composite) was used for comparison.

The phase constitutions of the W-Cu-Cr composite powders and bulks were idetified by X-ray diffraction (XRD, RikaguD/max-3c) with Cu K_α radiation, and the scanning speed was 4°/min. The scanning electron microscopy (SEM, Nova 200 Nano SEM) and transmission electron microscopy (TEM, JEM-2100F) equipped with an energy dispersive spectroscopy (EDS) detector were employed to characterize the microstructure of composites. The morphology and volume of the worn scar were measured by the PS50 three-dimensional (3D) surface profilometer. A high-resolution X-ray photoelectron spectroscopy (XPS, Kratos XSAM 800) was utilized to investigate the chemical state of the worn surface with spot size of 400 μm and pass energy of 30 eV. The analysis pressure of chamber was 2×10^{-7} Pa. The atom probe tomography (APT) characterizations were performed in a local electrode atom probe (CAMEACA LEAP 5000 XR). The required needle-shaped specimens were fabricated by lift-outs and annular milled in a FEI Scios focused ion beam/scanning electron microscope (FIB/SEM). Vickers hardness tester and nano-indentation instrument were used to measure the hardness of the sintered bulks and worn surfaces. The loading and unloading of indentation were finished in 15 s, and no holding time was used as reaching the load peak. The abrasion process with a total effective wear duration of 30 min was performed at room temperature. The load and a rotation speed are 80 N and 1000 r/min, respectively. The counterpart is Si_3N_4 ball with a diameter of 5 mm.

3. Results and discussion

3.1. Phase constitution and microstructure of W-Cu-Cr composites

XRD diffraction patterns of the W-Cu-Cr composite powders and bulks with different Cr contents are shown in Fig. 1. The diffraction peaks of W broaden gradually with the increasement of Cr content (Fig. 1a). It may be caused by large strain and obvious refinement of W powders. In addition, with increasing Cr contents, the right shift degree of W peak enhances gradually, indicating that more Cr dissolves in the W phase. The optimized SPS sintering process (970 °C, 100 MPa) was used to densify the W-Cu-Cr composite powders. It was found that the optimal sintering temperature is different for the W-Cu-Cr composite powders. The W-Cu-10Cr composite was prepared at a relatively lower sintering temperature of 955 °C because the Cu phase will flow out after sintering at 970 °C. From Fig. 1b, it can be found that the sintered bulks are composed of W and Cu phases, and no Cr peak was detected. The shift of W peak reveals that there is still a certain amount of Cr dissolved in the W phase. Furthermore, the dissolved Cr, which is verified by the shift degree of W peaks after sintering, in the W phase is proportional to the Cr content of addition. The diffraction peaks of W in the sintered composites are obviously narrower than those of the initial powders, indicating relief of strain and occurrence of grain growth during sintering process. After eliminating the strain effect, the grain sizes of W powders and bulks with different Cr contents were determined quantitatively by Scherrer Formula (Fig. 1c) [39]. It indicates that the addition of Cr has significant effect on stabilizing grain sizes of the composites after sintering. From the microstructures of the prepared W-Cu-Cr bulk composites with various Cr contents (Fig. S1 in the Supplementary Information), it was found that the size of W phase reduces with the increase of Cr content. This indicates that Cr can also refine the W phase in addition to the W grain size.

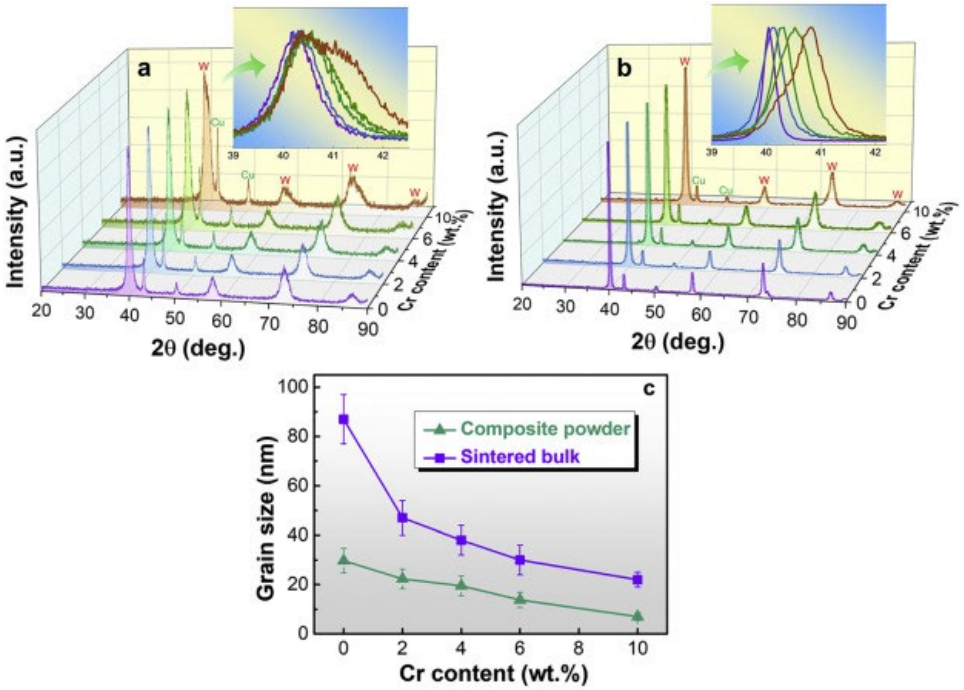

Fig. 1. Effect of Cr content on the phase constitutions of W-Cu-Cr composite powders (a) and sintered bulks (b), and variation of grain size of the composite powder and sintered bulk as increasing Cr content (c).

3.2. Hardness and wear resistance of W-Cu-Cr composites

Fig. 2a shows variation of relative density and hardness of the sintered composites. The relative density of the composite enhances with increasing Cr contents. At a content of 6 wt%Cr, the relative density of the composite reached a maximum of 96.79%. The hardness of composite still increased with Cr addition, although the relative density is reduced. It can be attributed to the refinement of phase and grain size of W (Fig. 1c) and further Cr dissolution in W (Fig. 1b). Moreover, the W-Cu-Cr composites was hardened obviously as increasing Cr content. The highest hardness of 1085 HV_{30} was achieved at a content of 10 wt% Cr.

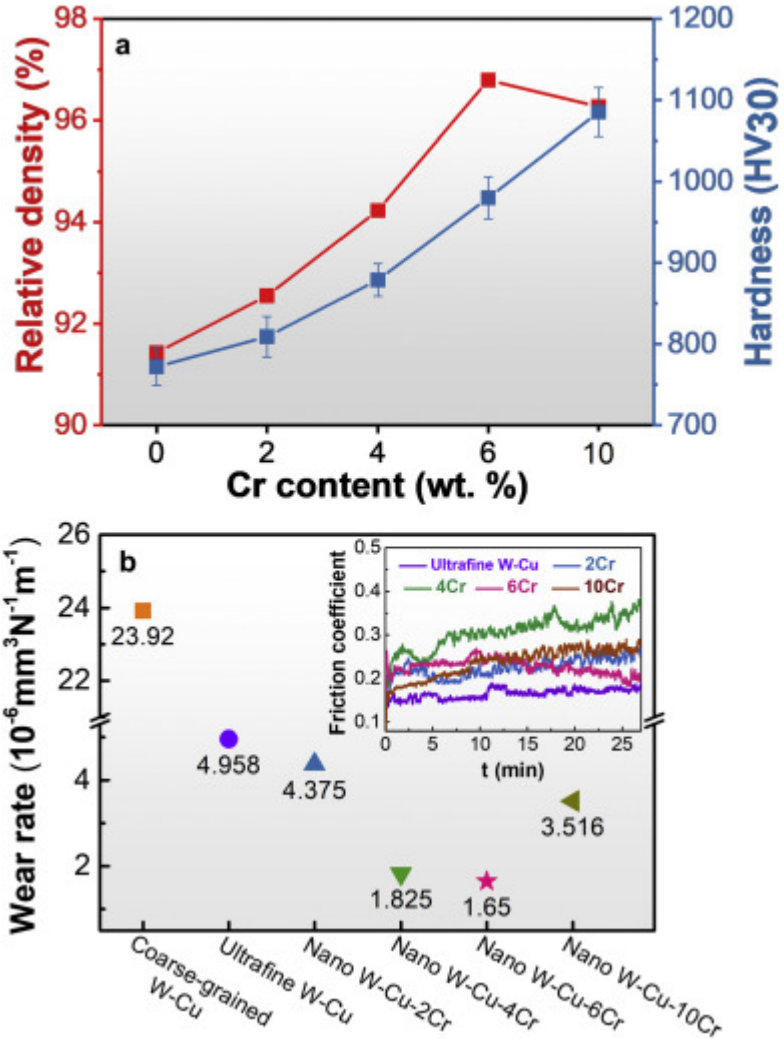

Fig. 2. Effects of Cr content on the relative density and Vickers hardness (a) and volumetric wear rate (b) of the W-Cu composites. The friction coefficients of composites with and without Cr are shown in the inset of (b).

To better evaluate the impact of refining microstructure and Cr addition on the wear resistance, coarse-grained W-Cu composite was also measured for comparison. Variations of volumetric wear rate with Cr content reveals that the wear resistance is improved firstly then reduced, showing a nonmonotonic variation trend with increasing hardness (Fig. 2b). The volumetric wear rate of the W-Cu-6Cr composite is 1.65×10^{-6} $mm^3/(Nm)$, which is lower than one third of that of the ultrafine W-Cu

composite with a W grain size of 120 nm [38], and is greatly improved by more than an order of magnitude compared with that of coarse-grained W-Cu composite. The variation of friction coefficient with different Cr contents is displayed in the inset of Fig. 2b. The friction coefficient of W-Cu composite is obviously smaller than that of the W-Cu-Cr composites. In the range of 0–4 wt% Cr addition, the friction coefficient gradually raises with the increase of Cr content. It can be attributed to the fact that the higher hardness has strong deformation resistance during the friction process. Further increasing Cr content should have enhanced friction coefficient at beginning of wear process. The higher friction coefficient also leads to raise in temperature and causes different oxidation behavior and microhardness at the worn surface. As a result, the W-Cu-6Cr and W-Cu-10Cr composites exhibit reduced friction coefficients compared with W-Cu-4Cr. However, the friction coefficient of the W-Cu-6Cr composite decreases gradually while that of the W-Cu-10Cr composite shows an opposite trend. It suggests that the wear modes of the composites are different.

3.3. Structure characterization of W-Cu-6Cr composite

The W-Cu-6Cr composite exhibits the highest relative density, good hardness and optimal wear resistance, indicating excellent comprehensive performance. Therefore, the W-Cu-6Cr composite was selected for further microstructure characterizations. The low magnification STEM image of W-Cu-6Cr composite and the distribution of Cu, Cr and W elements are presented in Fig. 3a-d. The Cr distributes mainly in the W phase, which can be attributed to the two-step ball milling process [38]. Moreover, because Cu and Cr elements are immiscible [40], the Cr can hardly dissolve into the Cu phase after sintering. In addition, the Cu phase keeps a good network structure and distribute evenly between the W phases, as shown in Fig. 3b. The high purity and connectivity of Cu phase are beneficial to maintaining good physical properties of the composite. From microstructure in the W phase observed by HAADF (Fig. 3e), the mean grain size of W is about 46 nm. We noticed a small amount of spherical precipitates with dark contrast formed at W grain boundary. HAADF image with high magnification (Fig. 3f) and elemental analysis (Fig. 3h, i) demonstrate that the precipitates are rich in Cr element. To further confirm the crystal structure and composition, HRTEM and fast Fourier transformation (FFT) analysis were performed (Fig. 3g). It was determined that the spherical precipitate is Cr-W-O ternary phase (PDF#43–0440) with a hexagonal structure. These precipitates were considered to form by substitution of some solute atoms for the matrix atoms, and may not have a precise composition as in a compound. The formation mechanism of these precipitates is related to the strong oxygen absorption capacity of Cr. During the phase separation process of W and Cr, the newly formed Cr-rich precipitates absorb oxygen to purify the grain boundary.

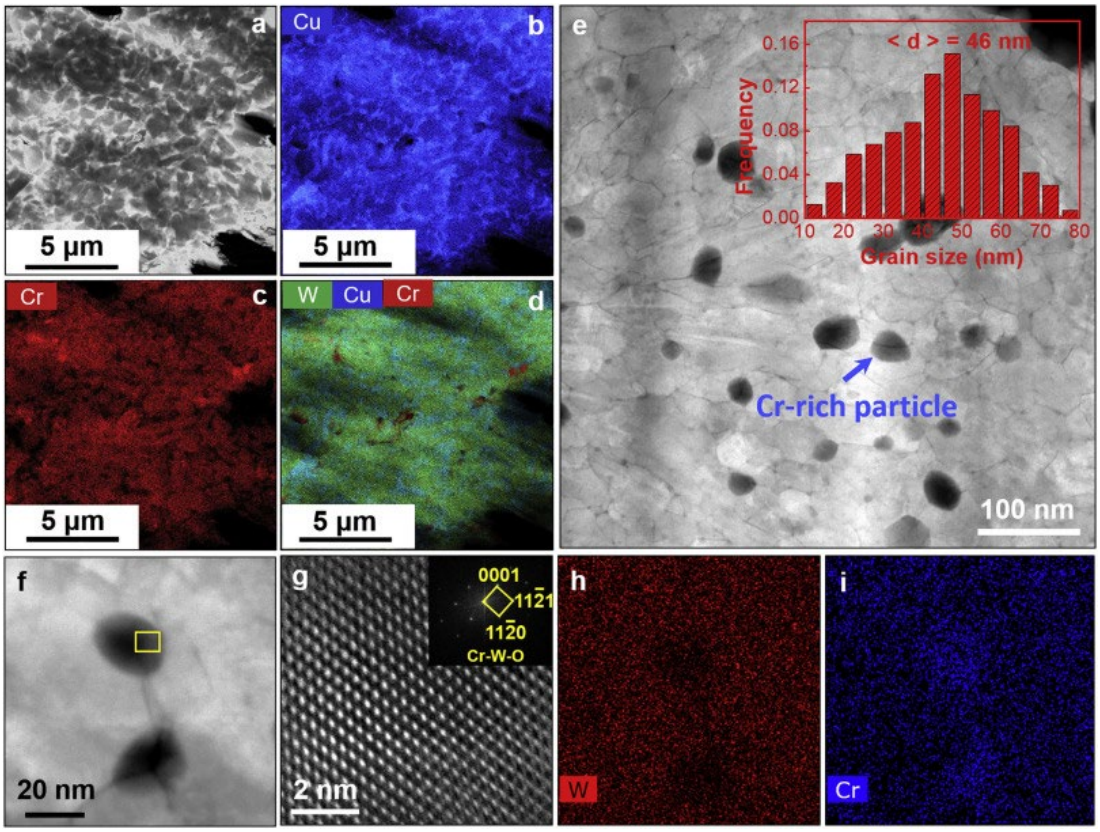

Fig. 3. Elemental distribution and nanocrystalline structure in the W grain of the W-Cu-6Cr composite: (a) Low magnification STEM image; (b-d) Distributions of Cu, Cr and W, respectively; (e) HAADF microstructure and grain size distribution of W grains; (f) HAADF image of precipitates and W grain boundaries; (g) HRTEM image and corresponding FFT of the precipitate; (h, i) Distributions of W and Cr.

To further reveal the mechanism of grain refinement of W grains, the nanostructure inside W phase was further characterized. The distributions of W and Cr at the triple junctions of grain boundaries is shown in Fig. 4a-d. The Cr and W elements coexist at W grain boundary, and the concentration of Cr element is significantly higher than that of W element, as indicated in Fig. 4c and d, indicating that the Cr element segregates at the interface in the form of thin film. During the mechanical alloying process, Cr dissolved in W grains and the supersaturated solid solution was formed. In the sintering process, a portion of Cr diffused from W grains and segregated at the grain boundaries, which reduced the interface energy. Therefore, in addition to pinning effect of these Cr-rich precipitates, the segregated Cr film at the grain boundaries inhibits effectively the growth of W grains and improves the thermal stability of the nanostructure during the sintering process.

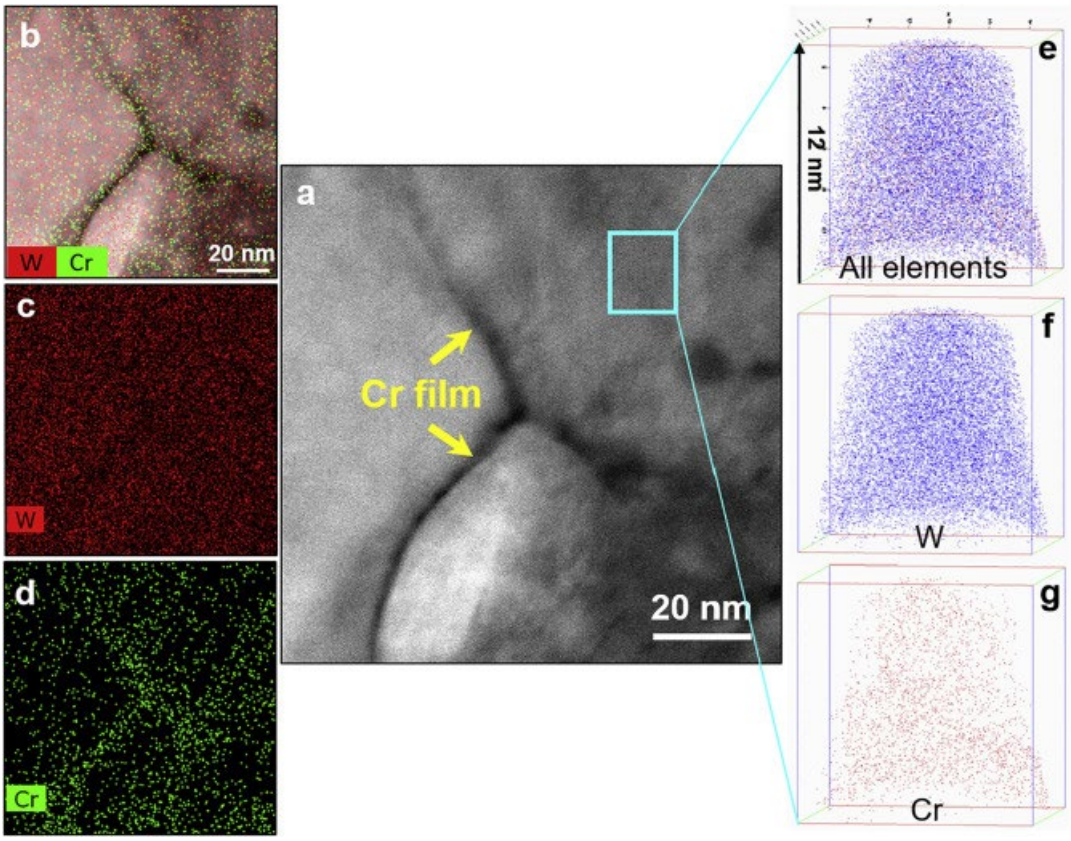

Fig. 4. Composition analysis at the triple junction of W grains in the W-Cu-6Cr composite: (a) HAADF image; (b-d) Distributions of W and Cr in (a); (e-g) Spatial distributions of W and Cr in the W grain characterized by APT.

It is expected that the segregation of Cr and formation of Cr-rich nanoparticles also happen at the surface of W particles. The Cr-rich precipitates contact each other and form interparticle necks. From the phase diagram, at a temperature of 970 °C, the solubility of W in Cr is 8.0 at.% approximately. Therefore, the segregated Cr film and interparticle Cr necks are capable of dissolving and transporting W atoms, which plays a role as rapid diffusion channel between particles [41]. In this way, it is beneficial for filling the space between particles and thus the relative density is increased with increasing Cr content. This is consistent with the result of Fig. 2a.

A typical atomic structure taken at W grain boundary indicated in the Fig. 5a is displayed in Fig. 5b. The atoms at the grain boundary arrange irregularly. The 3D APT analysis (Fig. 4e-g) shows that Cr disperses homogenously in the W grains, confirming that about 5 at.% of Cr still dissolves in the W grains after sintering. The dissolved Cr plays a solid solution strengthening effect on the W matrix. In addition, only diffraction information of W phase was found from the Fig. 5a and the FFT pattern in Fig. 5c. It further proves that the element Cr exists in the form of solid solution in W grain.

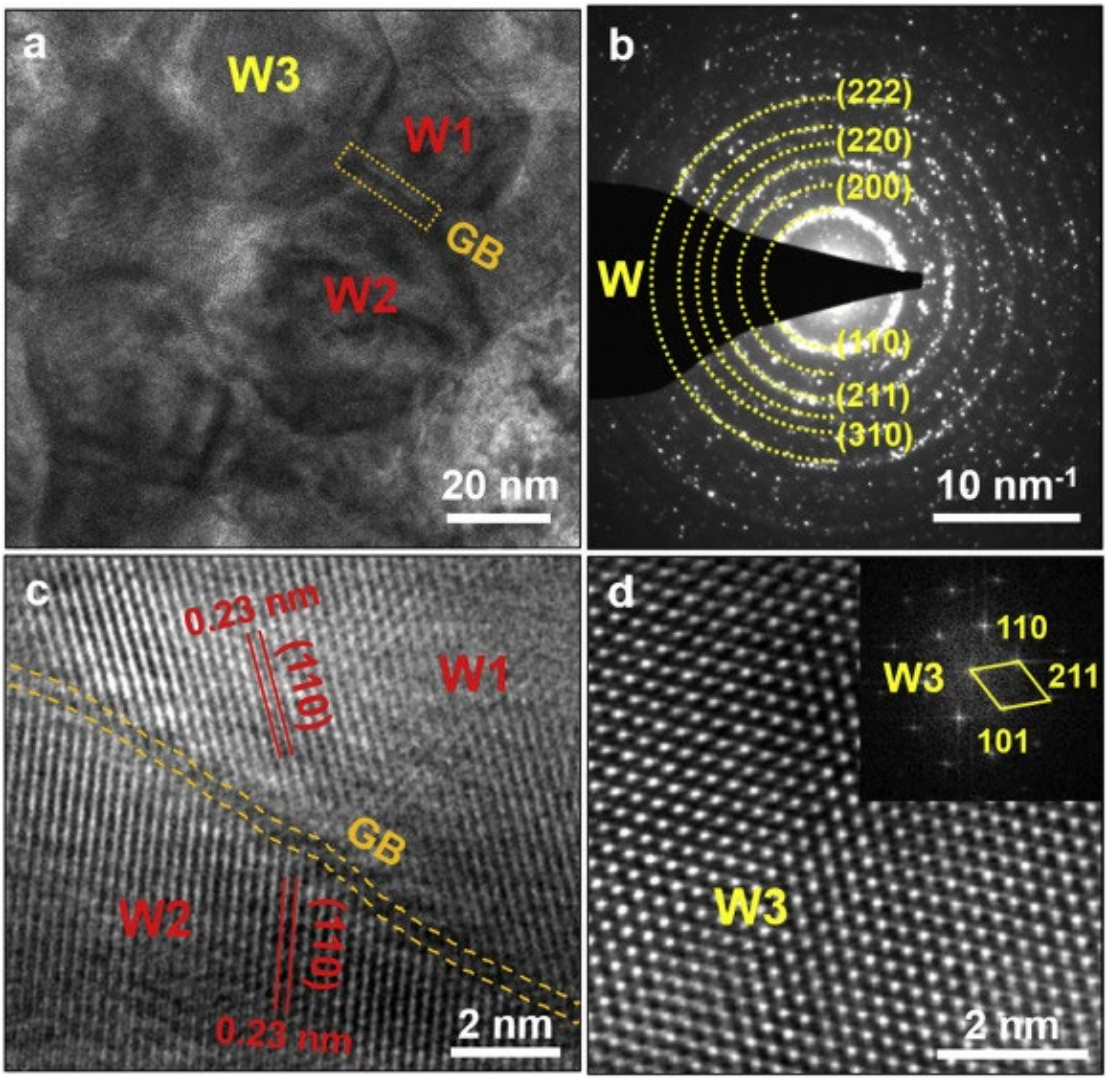

Fig. 5. Structural characterization in the W phase of the W-Cu-6Cr composite: (a) Morphology of W nanograins; (b) Diffraction patterns corresponding to the region in (a); (c) Grain boundary between W grains (W1 and W2); (d) HRTEM characterization of W3 grain in (a) and the corresponding FFT.

3.4. Evolution of composition and microstructure at the worn surface

The morphologies of the worn scar and the worn surface of coarse-grained W-Cu, ultrafine W-Cu and nanostructured W-Cu-6Cr composites were compared (Fig. 6). It is obvious that the wear volume of W-Cu composite is smaller than that of coarse-grained W-Cu composite (Fig. 6a, c), implying that the nanostructure in the W phase improves significantly the wear resistance of W-Cu composite. In addition, from the micromorphology with higher magnification (Fig. 6b, d), exfoliations and grooves can be found at the worn surfaces of ultrafine W-Cu and coarse-grained W-Cu bulk composites. The exfoliations result from partial fatigue failure of mechanical mixed layer (MML) caused by the continuous reciprocating slide load. Lots of grooves were produced along the sliding direction (SD) due to the scratch of those worn debris fallen off during the wear process. It can be concluded that the wear mode of binary W-Cu

composite is mainly abrasive wear and exfoliations, which is consistent with the result reported previously by our group [31].

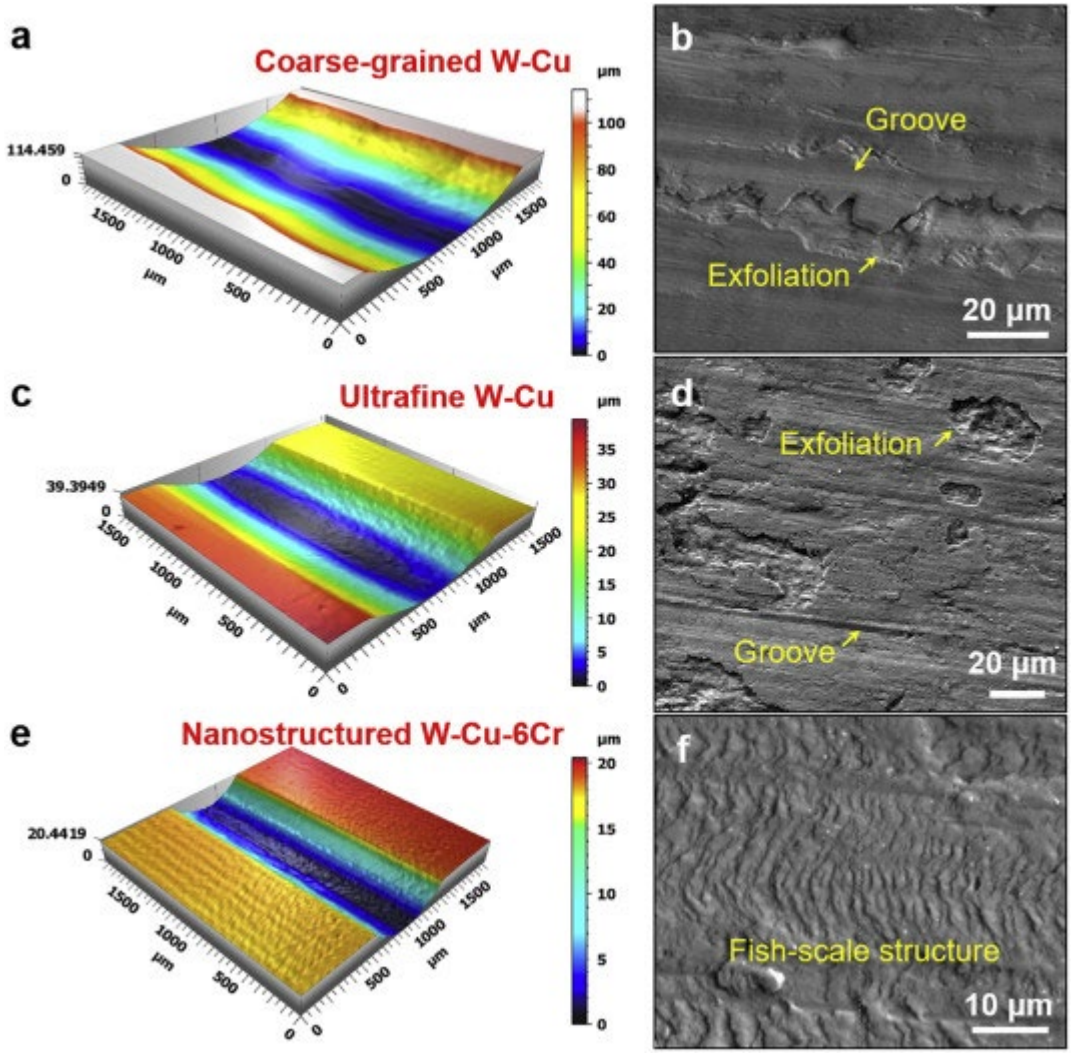

Fig. 6. Comparison on the morphologies of the worn scar and worn surface of different composites: (a, b) Coarse-grained W-Cu; (c, d) Ultrafine W-Cu; (e, f) Nanostructured W-Cu-6Cr.

As for the W-Cu-6Cr composite, fish-scale morphologies perpendicular to SD with a small number of grooves can be observed at the worn surface. This structure increases the roughness of the wear surface and can be used to explain the higher friction coefficient of W-Cu-Cr composite compared to that of binary W-Cu composite. The formation of the fish-scale structure also implies that the worn surface of W-Cu-6Cr composite has a higher degree of hardening during the wear process, resulting in difficult plastic deformation compared with binary W-Cu composite. In addition, there are few grooves at the worn surface of W-Cu-6Cr composite (Fig. 6f), indicating that the worn debris fallen off from matrix and the material loss caused by the abrasive wear is vanishingly small.

XPS spectra of W 4*f* of W-Cu composite (Fig. 7a) shows that the W phase is mainly oxidized to WO_3 and WO_2 during the wear process. The atomic percentages of W^{6+} and

W^{4+} were evaluated to be 75.11 and 24.89 at.%, respectively. In addition, XPS spectra of W 4*f* and Cr 2*p* at the worn surface of the W-Cu-6Cr composite (Fig. 7 b, c) demonstrate that W phase exists in the form of W, WO_3, WO_2 and $CuWO_4$. Their atomic percentages are 36.14, 49.95, 8.29 and 5.62 at.%, respectively. On the other side, the Cr element was oxidized into Cr_2O_3 phase. It indicates that the formation of Cr_2O_3 can inhibit W phase from further oxidation during the wear process. Furthermore, nanoindentation was used to measure the microhardness of the worn scar (Fig. 7d). The worn surface of W-Cu-6Cr composite has a higher hardness (4.84 GPa) than that of W-Cu composite (2.45 GPa) under a load of 50 mN, exhibiting better resistance against plastic deformation during the friction process due to the reduction of oxidation degree of W phase induced by forming stiff Cr_2O_3 component.

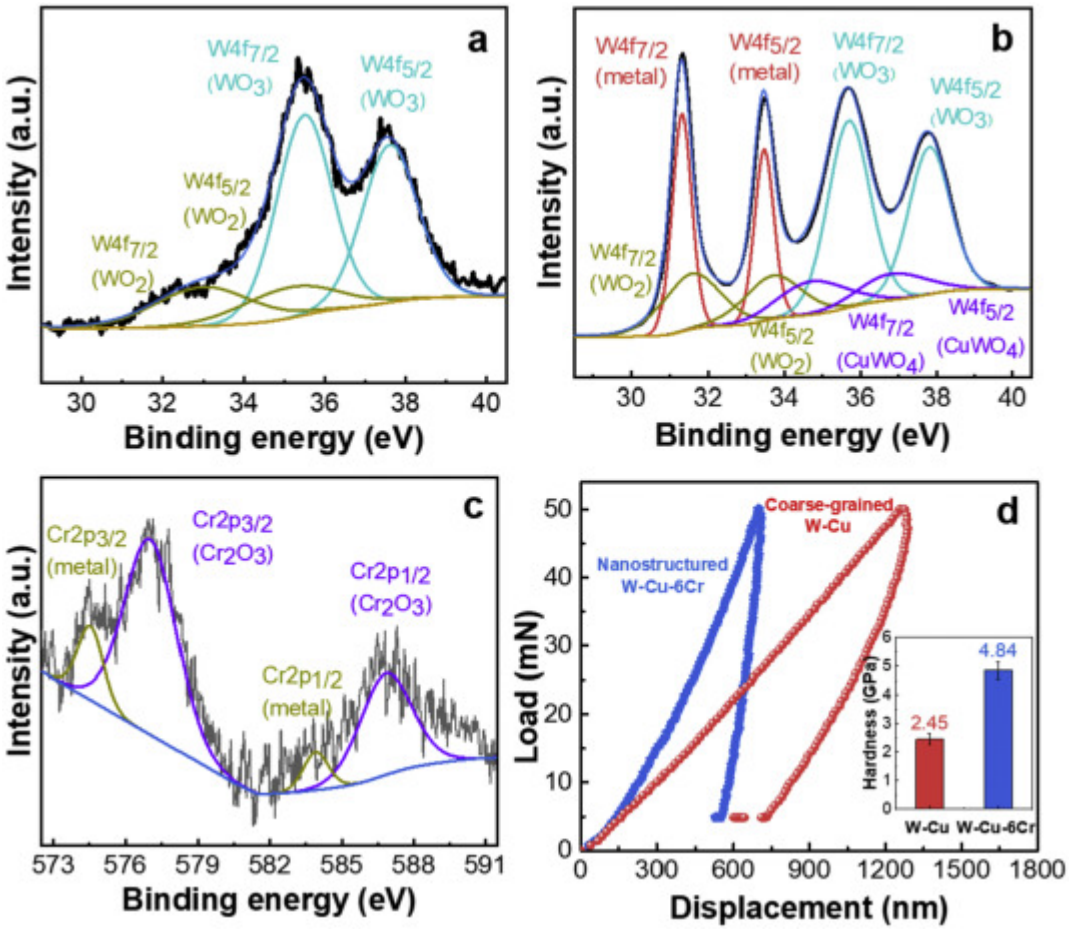

Fig. 7. XPS analysis and hardness test of different composites: (a) XPS spectra of W 4*f* at the worn surface of the W-Cu composite; (b, c) XPS spectra of W 4*f* and Cr 2*p* obtained from the worn track of the W-Cu-6Cr composites; (d) Load versus displacement curves of W-Cu and W-Cu-6Cr composites evaluated by nanoindentation. The hardness of the worn scar is shown in the inset of (d).

To reveal the microstructure evolution at the worn surface of the W-Cu-6Cr composite before and after wear process, FIB technology was used to extract a film sample from the worn scar along the SD. Detailed microstructure characterization and elemental distribution analysis under the worn scar are shown in Fig. 8. It can be seen that a dense

MML with a thickness of 0.5–1 μm was formed at the worn surface. W, Cr, O, and Cu elements distribute evenly in the MML observed from the EDS result, indicating that the dispersed W, Cr and Cu oxides are formed during the wear process. In addition, compared with the microstructure under the worn scar reported in the literature [31], there is restricted plastic deformation region below the MML of the W-Cu-6Cr composite. The above results reflect that the nanostructured W phase induced by the phase separation has strong resistance to plastic deformation. On the other hand, it also suggests that the worn surface undergoes a long-term reciprocating load, resulting in a sufficiently refined microstructure and a stable MML. The thickness of the oxide layer is much smaller than that of binary W-Cu composite (5–10 μm) reported in our previous work [31], indicating that the Cr addition prevents further oxidation into the deeper matrix. The above result is consistent with the XPS analysis.

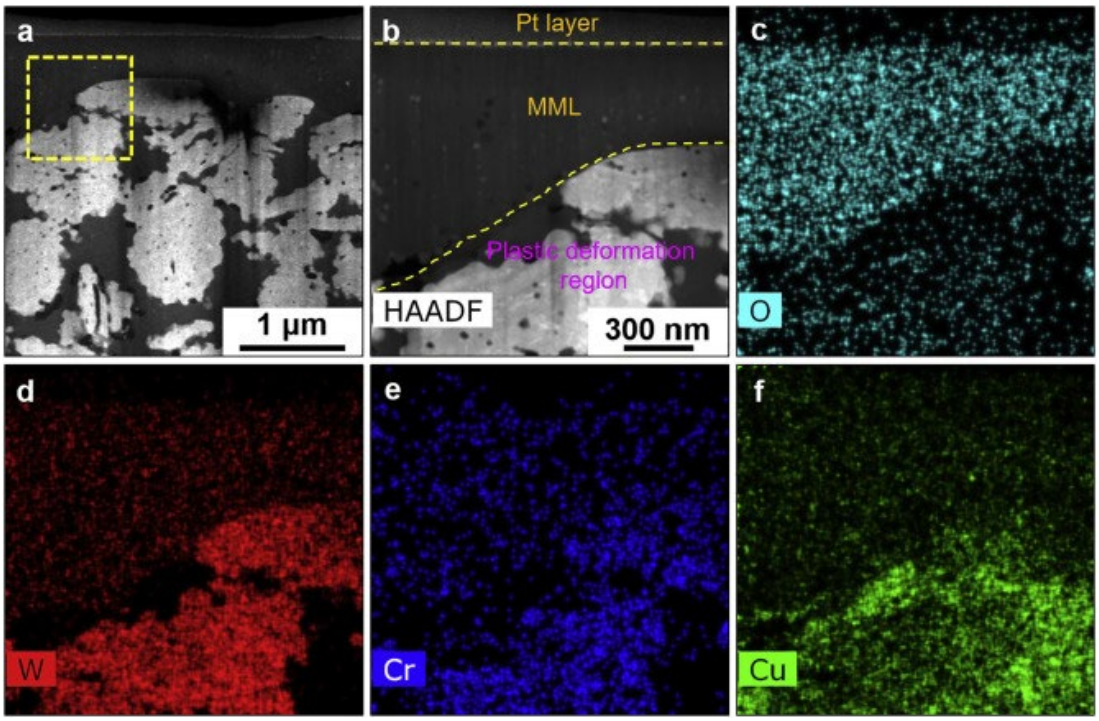

Fig. 8. Cross-sectional morphologies and elemental distributions beneath the worn surface of the W-Cu-6Cr composite: (a, b) HAADF morphologies with low and high magnifications; (c-f) The corresponding elemental distributions of O, W, Cr and Cu in (b).

The detailed cross-sectional microstructure of MML and plastic deformation region of W-Cu-6Cr composite (Fig. 9a) shows that the W grains in the plastic deformation region still maintains nanostructure, which endows the W phase with sufficient resistance to plastic deformation. Fig. 9b shows a 3D reconstruction map of an APT needle tip taken from the plastic deform region, which contains both W and dark precipitate. Proximity histogram across the interface gives a quantitative compositional analysis as shown in Fig. 9f. The atomic ratio of Cr and O in the dark precipitate is approximately 2:3, suggesting that the original Cr-W-O particles were oxidized to Cr_2O_3. The formation of the stable Cr_2O_3 particles is attributed to the adsorption of

oxygen from the oxide layer during the wear process, and further improves the resistance against plastic deformation of W phase.

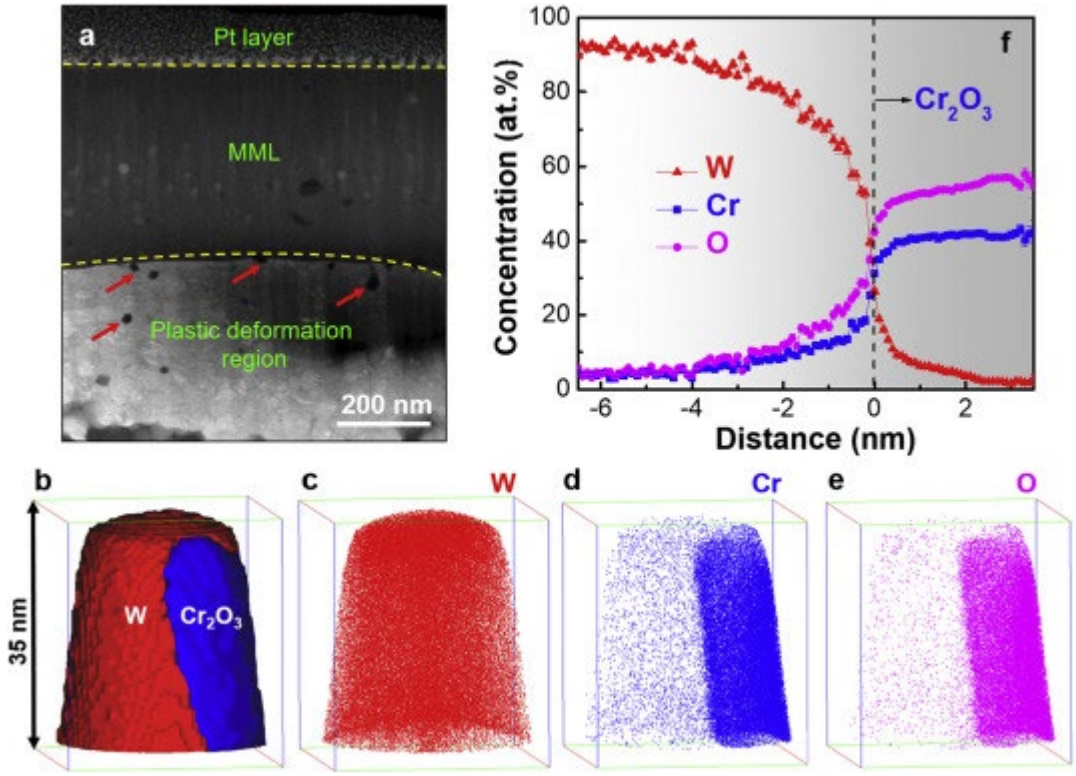

Fig. 9. Composition analysis of the particles with dark contrast in the plastic deformation region of the W-Cu-6Cr composite: (a) Cross-sectional microstructure of MML and plastic deformation region beneath the worn scar; (b) 3D reconstruction map of an APT needle tip containing W and dark precipitate. The isosurface with a concentration of 35% Cr was used to visualize the precipitate; (c-e) 3D atom maps of W, Cr and O; (f) Proximity histogram across the interface between the matrix and precipitate with dark contrast, giving a quantitative compositional analysis.

When the Cr content increases to 10 wt%, the wear resistance of W-Cu-10Cr composite reduces compared to that of W-Cu-6Cr composite (Fig. 2b). In order to explain this phenomenon, the microstructures of the W-Cu-6Cr and W-Cu-10Cr composites were compared (Fig. S2 in the Supplementary Information). When excessive Cr was introduced into the W-Cu composite, the distribution of Cr became inhomogeneous, and Cr-rich phases with larger sizes in a range of 200–500 nm formed at the adjacency between W phases.

The worn surface morphology of W-Cu-10Cr composite (Fig. 10a) indicates that the surface is relatively smooth and flat without exfoliation of delamination and grooves. The small roughness at the worn surface can be utilized to understand the lower friction coefficient than that of W-Cu-6Cr composite (inset of Fig. 2b). The microstructure and elemental distribution at the worn surface of the W-Cu-10Cr composite were also characterized to investigate the wear mechanism. Compared with the microstructure before wear process (Fig. 10b), the W phase is fragilized into fine particles after wear

process (Fig. 10c). It can be attributed to the higher concentration of Cr dissolved in the W grains and more Cr-rich precipitates located at the boundaries of W phases. Although the hardness of the W phase is improved significantly due to the Cr dissolution, excessive addition of Cr also leads to an increment in the brittleness. In addition, there are lots of regions with dark contrast among the brittle W particles as shown in Fig. 10c, which are determined to be "Cu pool" by EDS result of Fig. 10d-g. The oxygen content in these regions is much higher than that in the W phase. It verifies the improved oxidation resistance of W phase due to addition of Cr.

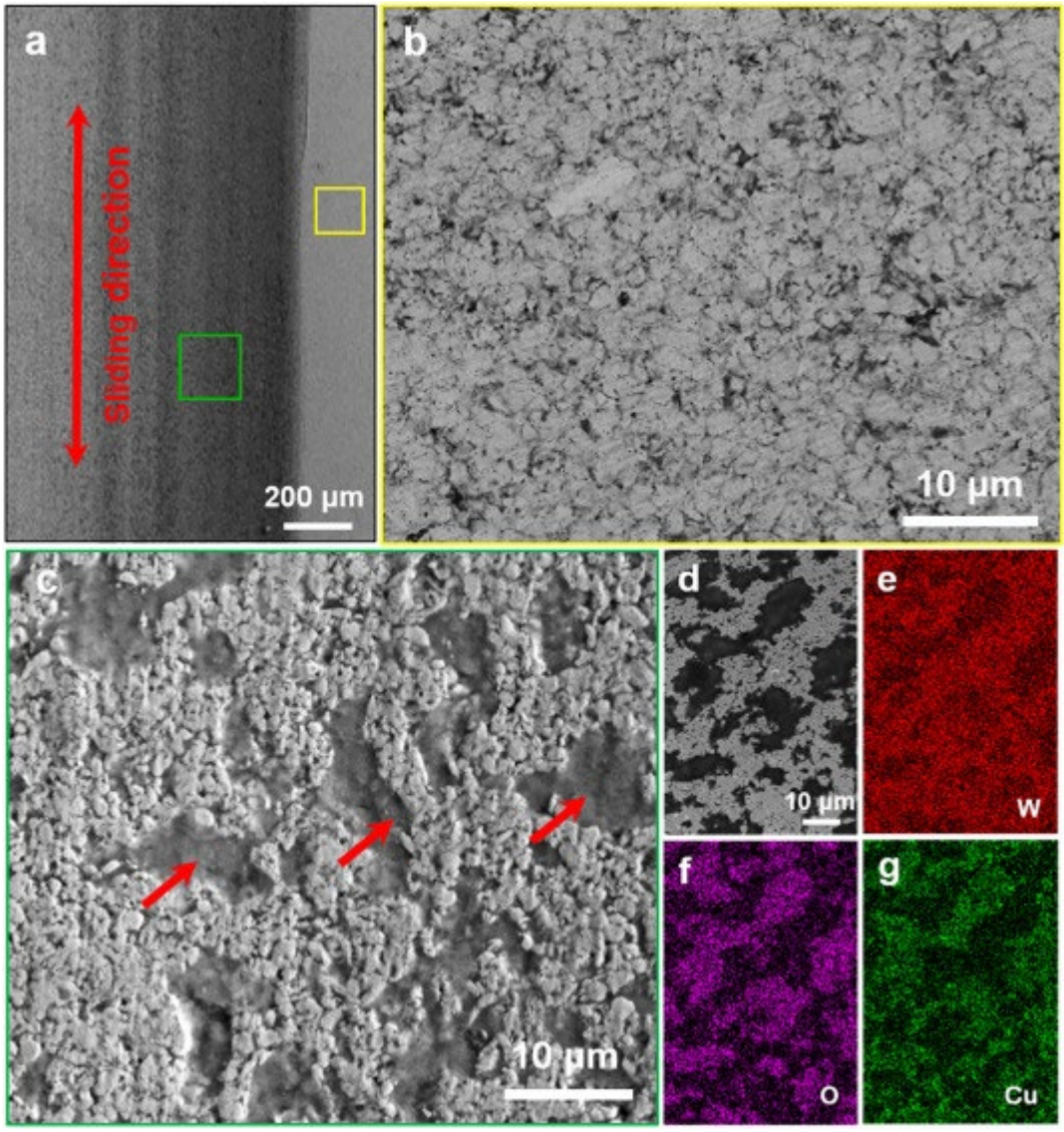

Fig. 10. Worn surface morphology and elemental distribution of the W-Cu-10Cr composite: (a) SEM morphologies of worn scar and matrix; (b) Microstructure of the matrix before wear process; (c, d) Microstructure at the surface of the worn scar; (e-g) Elemental distributions of W, O and Cu corresponding to the region in (d).

The W-Cu-10Cr composite has different wear behavior compared with W-Cu and W-Cu-6Cr composites. For the later, the broken W particles deform, forming a film spreading on the worn surface at the early stage of wear process. In this film, the W grains elongate along the wear direction [31,33]. After constant reciprocating sliding and oxidation, this film converts to protective MML with uniform composition and refined structure. The stable MML is beneficial for reducing the friction coefficient. However, excess Cr addition induces evident hardening even embrittlening of W. Deformation of W with grains elongation and spreading on the worn surface was restrained. The brittle W phases tend to break and redistribute under the reciprocating sliding load, resulting in the separated distribution of W and Cu phases. It is difficult to form MML with uniform composition and refined structure at the worn surface. Therefore, the wear resistance of W-Cu-10Cr composite was reduced compared with that of W-Cu-6Cr composite.

The W phase in the composite can be regarded as skeleton to resist further deformation in the process of loading. The comparative analysis of the microstructure and properties in terms of hardness and wear resistance of coarse-grained W-Cu and W-Cu-Cr composites shows that the nanostructured W phase can significantly improve the hardness and wear resistance of W-Cu-Cr composites. The mechanism of increment in the hardness can be attributed to the following three aspects: (I) Solid solution strengthening: The Cr can easily dissolve into the crystal lattice of W through high energy ball milling. Furthermore, partial Cr still remains in the W grain after sintering because of the rapid cooling process of SPS. Supersaturated Cr in the W phase plays the role of solid solution strengthening. (II) Dispersion strengthening: During the sintering process, the Cr tends to precipitate and in-situ react with oxygen to form a highly stable Cr-W-O nanoparticles at the W grain boundary. It plays an important role in purifying the grain boundary and preventing the movement of dislocations. (III) Fine grain strengthening: In addition to formation of Cr-W-O nanoparticle, the Cr also segregates at the grain boundaries of W to inhibit the grain growth of W effectively, leading to hindering the formation and movement of dislocations during the deformation process.

Besides, the wear resistance of W-Cu-Cr composites does not show a monotonous enhancement with increasing the hardness. There is an appropriate amount of Cr for achievement of optimal wear resistance. On one hand, the stable nanostructure of the W phase provides sufficient rigidity to resist plastic deformation. On the other hand, the Cr has an effect on the relief of W oxidation formation at the worn surface. As a result, a MML with relatively small thickness and fine dispersed W and oxide can be formed, which exhibits improved hardness compared with that of binary W-Cu composite and can prevent effectively subsequent wear. Although Cr is beneficial to increment in the hardness, excessive Cr deteriorates severely the toughness of the composite due to the supersaturation dissolution and inhomogeneous distribution of large Cr-rich phases located at the boundaries of W phases. It induces fragmentation of W phase and inhibits formation stable MML to protect the surface from further wear. As a result, the wear resistance of the W-Cu-10Cr composite decreases conversely.

4. Conclusions

The nanostructured W-Cu-Cr composites were fabricated through phase separation, and its wear resistance was investigated. The wear mechanisms with different microstructures and Cr contents were revealed based on the analysis of the composition, structural features and microhardness at the worn surfaces. The main conclusions are summarized as follows.

(1) In addition to supersaturated dissolution in the W phase, partial Cr atoms separate from W to form segregated films at grain boundaries, which inhibit the growth of W grains during the sintering process. As a result, the average W grain size was reduced to 46 nm in the W-Cu-Cr composite bulk. The segregated Cr absorbed oxygen and in-situ transformed into Cr-W-O phase, which distributed at W grain boundaries.

(2) The hardness of the W-Cu composite was significantly improved to 1085 HV through the combined effects of the refined grain size, solid solution of Cr and Cr-rich particles distributed at the grain boundaries. It is confirmed that nanostructuring of the W phase hence the improved resistance against plastic deformation of the W skeleton play a significant role in the high hardness of the composite.

(3) Nonmonotonic variation trend between the wear resistance and the hardness was discovered in the nanostructured W-Cu-Cr composites. The wear resistance of the W-Cu-6Cr composite was an order of magnitude higher than that of the coarse-grained W-Cu composite. Under the reciprocating sliding load, the preferential oxidation of Cr reduced the oxidation of W, and the nanostructure facilitated the formation of a stable protective film with refined structure and high hardness at the surface.

Declaration of Competing Interest

We declare that we do not have any commercial or associative interest that represents a conflict of interest in connection with the work submitted.

Acknowledgements

This work was supported by the National Natural Science Foundation of China (51631002, 51701007 and 51621003) and the International Cooperation Seed Fund of Beijing University of Technology (No. 2021B26).

References

[1] L. Dong, M. Ahangarkani, W. Chen, Y. Zhang, Recent progress in development of tungsten-copper composites: fabrication, modification and applications, Int. J. Refract. Met. Hard Mater. 75 (2018) 30–42.

[2] E. Tejado, A. Müller, J.H. You, J.Y. Pastor, Evolution of mechanical performance with temperature of W/Cu and W/CuCrZr composites for fusion heat sink applications, Mater. Sci. Eng. A 712 (2018) 738–746.

[3] P. Jayashree, S. Turani, G. Straffelini, Effect of testing conditions on the dry sliding behavior of a Cu-based refractory composite material, Tribol. Int. 140 (2019)

105850.

[4] W. Hu, Q. Ma, Z. Ma, Y. Huang, Z. Wang, Y. Liu, Ultra-fine W-Y2O3 composite powders prepared by an improved chemical co-precipitation method and its interface structure after spark plasma sintering, Tungsten 1 (2019) 220–228.

[5] Y. Huang, X. Zhou, N. Hua, W. Que, W. Chen, High temperature friction and wear behavior of tungsten-copper alloys, Int. J. Refract. Met. Hard Mater. 77 (2018) 105–112.

[6] Q. Chen, L. Li, X. Man, H. Sui, J. Liu, S. Guo, et al., In-situ synthesis of core-shell structure W(WC) composite grains in W-Cu composites fabricated by infiltration, J. Alloys Compd. 864 (2021) 158633.

[7] H. Zhou, K. Feng, Y. Xiao, Y. Liu, S. Ke, Pressure effects on a novel W-Mo-Cu alloyby large current electric field sintering: sintering behavior, microstructure and properties, J. Alloys Compd. 785 (2019) 965–971.

[8] B. Li, Z. Sun, G. Hou, P. Hu, F. Yuan, Fabrication of fine-grained W-Cu composites with high hardness, J. Alloys Compd. 766 (2018) 204–214.

[9] E. Svanidze, T. Besara, M.F. Ozaydin, C.S. Tiwary, J. Wang, S. Radhakrishnan, et al., High hardness in the biocompatible intermetallic compound β-Ti3Au, Sci. Adv. 2 (2016) 1–6.

[10] D.A. Rigney, Transfer, mixing and associated chemical and mechanical processes during the sliding of ductile materials, Wear 245 (2000) 1–9.

[11] T.J. Rupert, C.A. Schuh, Sliding wear of nanocrystalline Ni-W: structural evolution and the apparent breakdown of Archard scaling, Acta Mater. 58 (2010) 4137–4148.

[12] G. Christian, G. Johanna, G. Peter, Solids under extreme shear: friction-mediated subsurface structural transformations, Adv. Mater. 31 (2019) 1806705.

[13] F. Ren, S.N. Arshad, P. Bellon, R.S. Averback, M. Pouryazdan, H. Hahn, Sliding wear-induced chemical nanolayering in cu-ag, and its implications for high wear resistance, Acta Mater. 72 (2014) 148–158.

[14] W. Wu, C. Hou, L. Cao, X. Liu, H. Wang, H. Lu, et al., High hardness and wear resistance of W-Cu composites achieved by elemental dissolution and interpenetrating nanostructure, Nanotechnology 31 (2020) 135704.

[15] J.F. Curry, T.F. Babuska, T.A. Furnish, P. Lu, D.P. Adams, A.B. Kustas, et al., Achieving ultralow wear with stable nanocrystalline metals, Adv. Mater. 30 (2018)

1–7.

[16] A. Li, I. Szlufarska, How grain size controls friction and wear in nanocrystalline metals, Phys. Rev. B 92 (2015) 1–8.

[17] D. Liu, Q. Zhang, L. Zhuo, Y. Zhang, Y. Wang, J. Xu, Ultrafine-grained W-Cu-SiC composites prepared by mechanical alloying and infiltration of copper into pre-sintered skeleton, Powder Metall. 63 (2020) 180–186.

[18] M. Lou, X. Chen, K. Xu, Z. Deng, L. Chen, J. Lv, et al., Temperature-induced wear transition in ceramic-metal composites, Acta Mater. 205 (2020) 116545.

[19] Z. Iqbal, N. Merah, S. Nouari, A.R. Shuaib, N. Al-Aqeeli, Investigation of wear characteristics of spark plasma sintered W-25wt%Re alloy and W-25wt%Re-3.2wt %HfC composite, Tribol. Int. 116 (2017) 129–137.

[20] C. Hou, X. Song, F. Tang, Y. Li, L. Cao, J. Wang, et al., W-Cu composites with submicron-and nanostructures: progress and challenges, NPG Asia Mater. 11 (2019) 74–94.

[21] C. Chen, R. Pokharel, M. Brand, E. Tegtmeier, B. Clausen, D. Dombrowski, et al., Processing and consolidation of copper/tungsten, J. Mater. Sci. 52 (2017) 1172–1182.

[22] A. Devaraj, W. Wang, R. Vemuri, L. Kovarik, X. Jiang, M. Bowden, et al., Grain boundary segregation and intermetallic precipitation in coarsening resistant nanocrystalline aluminum alloys, Acta Mater. 165 (2019) 698–708.

[23] T. Huang, A.R. Kalidindi, C.A. Schuh, Grain growth and second-phase precipitation in nanocrystalline aluminum-manganese electrodeposits, J. Mater. Sci. 53 (2018) 3709–3719.

[24] T. Chookajorn, H.A. Murdoch, C.A. Schuh, Design of stable nanocrystalline alloys, Science 337 (2012) 951–954.

[25] H.A. Murdoch, C.A. Schuh, Stability of binary nanocrystalline alloys against grain growth and phase separation, Acta Mater. 61 (2013) 2121–2132.

[26] L. Cao, C. Hou, F. Tang, S. Liang, J. Luan, Z. Jiao, et al., Thermal stability and high-temperature mechanical performance of nanostructured W-Cu-Cr-ZrC composite, Compos. Part B 208 (2020) 108600.

[27] W. Daoush, J. Yao, M. Shamma, K. Morsi, Ultra-rapid processing of high-hardness tungsten-copper nanocomposites, Scr. Mater. 113 (2016) 246–249.

[28] X. Li, P. Hu, J. Wang, S. Chen, W. Zhou, In situ synthesis of core-shell W-Cu nanopowders for fabricating full-densified and fine-grained alloys with dramatically improved performance, J. Alloys Compd. 853 (2021) 156958.

[29] T. Mik´o, F. Krist´aly, D. Peth, M. Sveda, G. Karacs, G. Gergely, et al., Investigation of nanocrystalline sintered W-25 wt% Cu composite, Int. J. Refract. Met. Hard Mater. 95 (2020) 105438.

[30] L. Wan, J. Cheng, Y. Fan, Y. Liu, Z. Zheng, Preparation and properties of superfine W-20Cu powders by a novel chemical method, Mater. Des. 51 (2013) 136–140.

[31] C. Hou, L. Cao, Y. Li, F. Tang, X. Song, Hierarchical nanostructured W-Cu composite with outstanding hardness and wear resistance, Nanotechnology 31 (2019), 084003.

[32] L. Sun, G. Wu, Q. Wang, J. Lu, Nanostructural metallic materials: structures and mechanical properties, Mater. Today 38 (2020) 114–135.

[33] Y. Li, C. Hou, L. Cao, C. Liu, S. Liang, F. Tang, et al., Excellent wear resistance of multicomponent nanocrystalline W-Cu based composite, J. Alloys Compd. 861 (2021) 158627.

[34] F.I. Danilov, V.S. Protsenko, V.O. Gordiienko, S.C. Kwon, J.Y. Lee, M. Kim, Nanocrystalline hard chromium electrodeposition from trivalent chromium bath containing carbamide and formic acid: structure, composition, electrochemical corrosion behavior, hardness and wear characteristics of deposits, Appl. Surf. Sci. 257 (2011) 8048–8053.

[35] W. Zhu, C. Zhao, Y. Zhang, C. Kwok, J. Luan, Z. Jiao, et al., Achieving exceptional wear resistance in a compositionally complex alloy via tuning the interfacial structure and chemistry, Acta Mater. 188 (2020) 697–710.

[36] Q. Zhang, S. Liang, L. Zhuo, Ultrafine-grained W-25wt.%Cu composite with superior high-temperature characteristics, Mater. Sci. Technol. 33 (2017) 2071–2077.

[37] K. Lu, L. Lu, S. Suresh, Strengthening materials by engineering coherent internal boundaries at the nanoscale, Science 324 (2009) 349–352.

[38] L. Cao, C. Hou, Y. Li, X. Liu, S. Liang, X. Song, Novel nanocrystalline W-Cu-Cr-ZrC composite with ultra-high hardness, Nanotechnology 31 (2020) 134002.

[39] A.L. Patterson, The Scherrer formula for X-ray particle size determination, Phys. Rev. 56 (1939) 978–982.

[40] C. Qiu, B. Hu, J. Zhou, P. Wu, Y. Liu, C. Wang, et al., The phase equilibria of the Cu-Cr-Ni and Cu-Cr-Ag systems: experimental investigation and thermodynamic modeling, CALPHAD 68 (2020) 101734.

[41] M. Park, C.A. Schuh, Accelerated sintering in phase-separating nanostructured alloys, Nat. Commun. 6 (2015) 6858.